

# Improving Spectrum Efficiency of Cell-Edge Devices by Incentive Architecture Applications With Dynamic Charging

Jinsong Gui , Member, IEEE, Lihuan Hui, Neal N. Xiong , Senior Member, IEEE, and Jie Wu , Fellow, IEEE

**Abstract**—The gap between the peak-hour Internet and the average level is increasing, which inevitably creates a type of temporary cellular weak coverage when there is a surge in data traffic demand, where any cell-edge device will have a low spectrum efficiency (SE). In this article, we propose a novel incentive architecture based on the dynamic radio frequency charging technology to improve the SE and use the Stackelberg game theory to formulate the problem. In such a model, a small base station (SBS) acts as the leader to offer a desired partition of the resource block obtained by a cell-edge device, while some small energy providers (SEPs) and small virtual access points (SVAPs) that are selected from user equipment act as the followers to make their decisions, respectively, to compete for the free part of such a resource block. Following the potential game rules, all the SEPs compete for a specific free resource part allocated by the SBS, and then, all the SVAPs compete for another nonoverlapping part allocated by the SBS on the basis of the results of the SEPs' potential game. Although our incentive architecture formally has three game stages, it is essentially a two-level Stackelberg game, which is analyzed by using a backward induction method. The theoretical analysis proves the convergence of the above-mentioned game models, and the simulation results demonstrate that the proposed incentive architecture can improve the SE for each cell-edge device.

**Index Terms**—Cell-edge device, dynamic charging, incentive architecture, spectrum efficiency (SE).

## I. INTRODUCTION

**P**EAK Internet traffic during busy periods is growing faster than the average level and the gap is widening [1]. In addition, tablets, smartphones, and machine-to-machine (M2M) [2],

Manuscript received April 6, 2020; accepted April 6, 2020. Date of publication April 13, 2020; date of current version November 18, 2020. This work was supported by the National Natural Science Foundation of China under Grant 61873352 and Grant 61272494. Paper no. TII-20-0547. (Corresponding author: Neal N. Xiong.)

Jinsong Gui and Lihuan Hui are with the School of Computer Science and Engineering, Central South University, Changsha 410083, China (e-mail: jsgui06@163.com; mltsuan@163.com).

Neal N. Xiong is with the Department of Mathematics and Computer Science, Northeastern State University, Tahlequah, OK 74464 USA (e-mail: xionгнаixue@gmail.com).

Jie Wu is with the Center for Networked Computing, Temple University, Philadelphia, PA 19122 USA (e-mail: jjewu@temple.edu).

Color versions of one or more of the figures in this article are available online at <https://ieeexplore.ieee.org>.

Digital Object Identifier 10.1109/TII.2020.2987089

[3] traffic will exceed fixed IP traffic in the near future. Besides enhanced mobile broadband applications, a major driver of this growth will come from increasing demand in the consumer wearable market and the wearable medical devices market. In 2017, the global wearable medical devices market was estimated to be worth \$5.2 billion, which is expected to increase to \$13.5 billion in 2022 [4].

## A. Motivation

An effective way for mobile operators to cope with explosive traffic growth is to build ultradense wireless access networks, where many microcells are overlapping in each macrocell, and in turn, many pico/femto cells are overlapping in each microcell. In fact, mobile operators are reluctant to deploy ultradense networks seamlessly and universally to meet peak traffic demand, since the increasing gap between peak traffic and the average level will lead to a decreasing utilization rate of their invested equipment/devices. Areas such as sports venues, expo centers, and industrial parks on the outskirts are not usually covered in an ultradense manner. However, spontaneous events, such as folk sports events, festival celebration activities, and large-scale commodity fairs, may be held in these places from time to time. Thus, a type of weak cellular coverage area is inevitably formed, where the resource utilization rate will be much worse if the limited resources are obtained by cell-edge devices.

For noncell-edge devices, if they are eager to get access services but the corresponding access resources are not allocated to them, they will have an incentive to forward data of cell-edge devices as long as these cell-edge devices are willing to share their frequency bands with noncell-edge devices. Because such noncell-edge devices both forward the data of the cell-edge devices and send their own data, their battery lifetime will be significantly shortened, which is a critical issue to be resolved. Energy harvesting is a feasible solution for prolonging the battery lifetime of such energy-constrained wireless devices.

Radio frequency (RF) energy transfer and harvesting is a far-field energy transfer technique, which is suitable for powering a large number of wireless devices distributed in a wide area. However, RF transmission signal strength is attenuated by the distance between the transmitter and the receiver. When an RF energy harvester is far away from any dedicated RF source, its capture efficiency is extremely low. Some user equipment (UE)

with advantages in terms of energy reserve and the geographical position may be recruited as rechargers, where they will get free frequency bands in return as soon as they are willing to exchange.

Regarding wireless networking research involving the application of the RF energy transfer and harvesting technique, to the best of our knowledge, the authors in [5] were the first to combine RF energy compensation and free frequency band supply to design an incentive mechanism, where the UE are motivated to take on some network responsibilities to improve the network capacity in a weak cellular coverage area.

In [5], the additional frequency bands are used as rewards. However, in the scenario mentioned above, the frequency band resources are scarce, and thus, no additional frequency band is available. Additionally, only a single cellular interface is considered for utilization, and thus, energy transfer and information transmission need to be carried out in a time division multiple access (TDMA) manner, even if the used frequency bands do not overlap each other. Moreover, a base station is required to replenish energy for temporary relays, where a large amount of energy is wasted in the transmission path instead of being utilized by these temporary relays. Finally, due to the consideration of overlay communication mode, not only is the frequency band quantity insufficient, but the utilization rate is also too low. Therefore, these issues require further discussion.

### B. Our Key Contributions

We address the above-mentioned issues in this article, and the main contributions are listed as follows.

- 1) When a resource block (that is, a frequency band) is assigned to a cell-edge device, it cannot be fully utilized. Therefore, we focus on its spectral efficiency (SE) improvement. On the premise of ensuring the quality of application experience of a cell-edge device user, the rest of this resource block can be coordinated by a small base station (SBS) as the reward resources.
- 2) Radio interfaces such as Wi-Fi and Bluetooth have become the normal configuration of wireless devices, so we combine them with the cellular interface and integrate them into the solution design to make full use of nonoverlapping parts of the resource block.
- 3) By recruiting the UE that have advantages in energy reserve and geographical position as rechargers rather than depending on the SBS to provide RF energy, a large amount of energy will be harvested by temporary relays rather than wasted in the transmission path.
- 4) To achieve the above-mentioned goals, especially to improve the SE of each cell-edge device, we propose an incentive architecture based on dynamic charging and formulate the partition problem of the resource block of cell-edge devices as a Stackelberg game. The response strategies [i.e., Stackelberg Nash equilibrium (SNE)] of all the players can be achieved by running the set of proposed algorithms.

### C. Organizational Structure

The rest of this article is organized as follows. In Section II, we review related work. Section III–IV describe system model,

scheme statement, and the analysis of the proposed scheme, respectively. Section VI presents the design details for the algorithms with respect to the proposed scheme. Section VII evaluates the simulation results. Finally, Section VIII concludes this article.

## II. RELATED WORK

In this section, we mainly introduce the existing works regarding dynamic charging applications in wireless networks. [6] presented a comprehensive overview of the research progress in various wireless networks with RF energy harvesting capability, including network architecture, circuit design, communication protocol design, and existing applications.

Subsequently, many types of literature have focused on the application of RF energy harvesting technique in cellular networks. [7] considered the dynamics of wireless power transfer (WPT) and its impact on secrecy. [8] discussed the simultaneous wireless information and power transfer (SWIPT) problem and proposed a distributed power control scheme for receiving terminals. [9], introduced a power utility that captures the power cost at the base station and the used power from mobile terminals' batteries in cellular networks.

[10] explored a communication system with wireless energy transfer capability and proposed an algorithm to maximize the average uplink data rate. [11] addressed the energy efficiency maximization problem for downlink information and energy transfer. By jointly optimizing the power allocation proportions at the base station and power splitting (or time switching) factors at the receivers, the proposed scheme could both maximize the minimum transmission rate of all receivers and improve the power efficiency.

In addition to the application in cellular networks, the RF energy harvesting technique has been widely applied to wireless sensor networks. [12] applied multiple dedicated RF sources with a harvest-then-transmit protocol to wireless body sensor networks. [13] investigated a wireless-powered sensor network, including one power beacon and multiple sensor nodes. [14] surveyed a multiantenna technique similar to beamforming which helps resist signal decay in energy transfer.

[15] applied the SWIPT technique to a mobile wireless sensor network where the relay nodes harvest energy from ambient RF signals to compensate for the energy consumption of their forwarding data. [16] proposed a relay selection protocol which is used in an energy harvesting wireless body area network with buffer. [17] proposed a cooperative integration scheme of RF energy harvesting and dedicated WPT for wireless sensor networks where the power conversion efficiency (PCE) reaches more than 40% when the ambient energy ranges from  $-15$  to  $-10$  dBm, while it is more than 60% when dedicated power ranges from 10 to 15 dBm.

In addition, [18] presented a comprehensive methodology for modeling hybrid energy harvesting communication systems, and they also developed the system model with multiple energy sources (e.g., RF, light, heat, and vibration) for energy harvesting. In order not to affect information transmission performance under traditional licensed channels, [19] used a 5-GHz unlicensed channel as a dedicated wireless power transmission

medium to offload the sharing of traditional licensed channels, which is based on the licensed-assisted access protocol for transferring power and information.

[20] introduced an incentive mechanism into an RF energy harvesting-based Internet of Things (IoT) system, where charging sources are specifically deployed to provide recharging service. However, a huge investment is needed to build these charging sources. Due to limited budgets, a resource-limited operator operates either the data transmission service or the RF energy transfer service. To effectively motivate the collaboration between them, an effective incentive mechanism is required to improve their payoffs. Due to the high attenuation of RF energy transfer, [21] proposed an energy bank-based crowdsourcing framework and an incentive mechanism, which can conserve energy while guaranteeing that battery-powered devices will complete various tasks.

However, the above-mentioned works do not combine RF energy compensation and free frequency band supply to design the incentive mechanism for the purpose of improving cellular coverage quality. Unlike the above-mentioned works, [5] studied the concerned scenario and developed a game-theoretic framework for enhancing cellular coverage quality. However, as mentioned above, the shortcomings in [5] motivate us to continue to search for a new incentive architecture based on dynamic charging to improve the SE of cell-edge devices in this article.

Furthermore, in terms of the application of the incentive mechanism, our purpose is completely different from those of the above-mentioned incentive schemes. For example, the purpose in [20] is to motivate the dedicated recharging service providers to recharge sensors and pay these recharging service providers monetarily as a reward. The purpose in [21] is to motivate wireless devices to participate in crowdsourcing and pay these wireless devices energy as a reward. Our goal is to motivate UE to provide a recharging service or data relaying service and pay these UE the spectrum as a reward.

### III. SYSTEM MODEL

#### A. Network Architecture

As shown in Fig. 1, we consider a microcellular network that consists of a centrally located SBS and many UE that are randomly distributed among this area and no smaller cells overlap in the same area. To reduce interference to UE in adjacent microcells, the maximum transmission power of the SBS is usually limited. Additionally, the maximum transmission power of each UE is usually smaller than that of the SBS.

As stated in Section I, even if a cell-edge device (i.e., any UE in the gray region in Fig. 1) transmits data to the SBS by adopting its maximum transmission power, it is generally difficult for the SBS to achieve the desired low receiving bit error rate. Therefore, a set of small cell virtual access points (SVAPs) should be selected from the UE in the white region in Fig. 1 to act as data relaying nodes, which can reduce not only the transmission power of cell-edge devices but also the receiving bit error rate of the SBS. Moreover, a set of small cell energy providers (SEPs) should be selected from the UE in the same

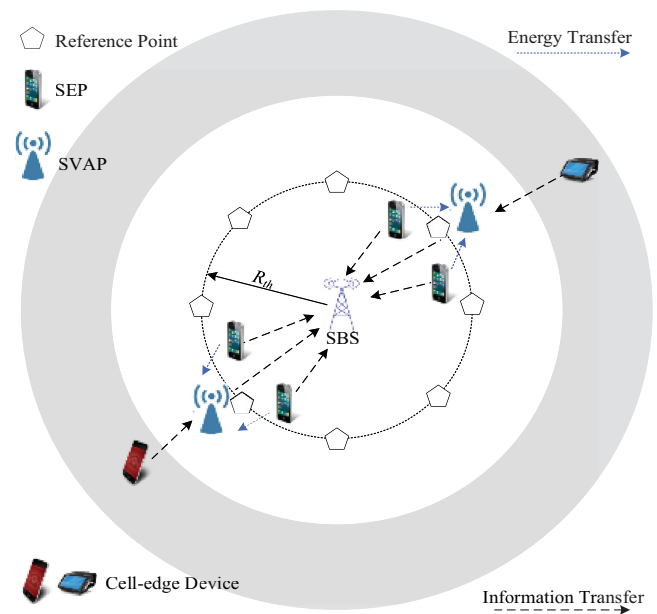


Fig. 1. Network architecture based on dynamic charging.

area to act as recharging nodes of SAVPs, which can prolong the lifetime of SVAPs.

In general, the SBS is responsible for the selection of SVAPs and SEPs. First, it sets up several reference points based on network deployment planning to assist the selection of SVAPs, which can ensure that the link quality between the selected SVAP and the SBS, and that between a cell-edge device and this SVAP, will not have a significant gap. The SBS achieves this goal by adjusting the parameter  $R_{th}$  in Fig. 1.

The UE that can replace a reference point to act as a SAVP needs to satisfy the following conditions.

- 1) It should be equipped with the common types of wireless interfaces (e.g., LTE, Wi-Fi, and Bluetooth).
- 2) It should guarantee that it will not move at a given time.
- 3) It wants to communicate with the SBS but currently does not have the required communication resources.
- 4) It should be capable of capturing RF energy.
- 5) It should be closest to this reference point among all the UE that satisfy the first four conditions.

After determining a set of the desired SVAPs, for each SVAP, the SBS will select a set of the SEPs for it. The UE that can be selected as a SEP needs to satisfy the following conditions.

- 1) It should guarantee that it will not move at a given time.
- 2) It wants to communicate with the SBS but does not have the required communication resources.
- 3) It should have an energy reserve that is not less than a given threshold.
- 4) It should have a line-of-sight transmission link with this SVAP.
- 5) It should be closest to this SVAP among the UE which satisfy the first four conditions.

Due to the limited space, this article will not discuss the specific selection algorithms for SVAPs and SEPs. However, a set of similar algorithms as in [5] can be used in this article

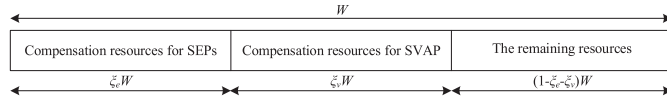


Fig. 2. Resource block partitioning for a cell-edge device.

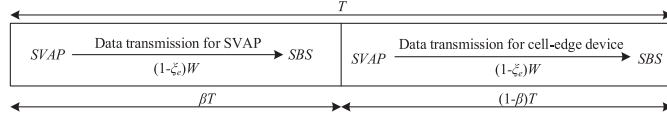


Fig. 3. Structure of the time frame for a SVAP.

as long as the above-mentioned selection conditions are strictly enforced.

Any cell-edge device can also associate itself with the SAVP that has the best channel condition between them using the UE association algorithm in [5]. By the corresponding algorithms in [5], the SBS (e.g.,  $s$ ) will get the *set* of SVAPs (e.g.,  $S_s$ ), while any SVAP (e.g.,  $v$ ) in  $S_s$  will get the *set* of SEPs (e.g.,  $R_v$ ) and the *set* of associated UE (e.g.,  $U_v$ ).

### B. Time-Slotted Scheme

Suppose that the SBS adopts the fixed number of orthogonal subcarriers to communicate with each UE, where the total frequency band of any UE is called as a resource block and denoted as  $W$ . In this article, we focus on how to improve the utilization of such a resource block  $W$  when it is allocated by the SBS to a cell-edge device.

The SBS divides the resource block  $W$  into three parts as shown in Fig. 2, where  $\xi_e W$  is used to compensate for a set of SEPs that recharge for the specified SVAP and  $\xi_v W$  is used to compensate for the specified SVAP that relays the data of this cell-edge device. The parameters  $\xi_e$  and  $\xi_v$  are the bandwidth partition coefficients for the SEPs and the SVAPs, respectively, where  $0 \leq \xi_e \leq 1$  and  $0 \leq \xi_v \leq 1$ , but usually  $1 - \xi_e - \xi_v$  should be not less than zero.

To receive the data from  $|S_s|$  SVAPs and  $|S_s||R_v|$  SEPs simultaneously, we suppose that the SBS is at least equipped with  $|S_s| + |S_s||R_v|$  antennas. Usually, each of all the UE is furnished with one cellular antenna, one Wi-Fi antenna, and one Bluetooth antenna. In this article,  $|\cdot|$  denotes the number of members in a *set*. For example,  $|R_v|$  is the number of SEPs in  $R_v$ , while  $|S_s|$  is the number of SVAPs in  $S_s$ .

Since each SVAP is only furnished with one cellular antenna, its cellular communication time is divided by the SBS into time frames that are repeated and have the same length (e.g.,  $T$ ). For any specified SVAP (e.g.,  $v$  in  $S_s$ ), the SBS specifies the structure of each time frame shown in Fig. 3, which includes two time slots—a time slot (i.e., during the  $\beta T$  time and  $0 < \beta < 1$ ) is used to send its own data over the frequency band  $(1 - \xi_e)W$ , while the other one (i.e., during the  $(1 - \beta)T$  time) is used to forward the data of the cell-edge device over the same frequency band.

We stipulate that any SVAP receives the data from its associated cell-edge device through the Bluetooth antenna, while it

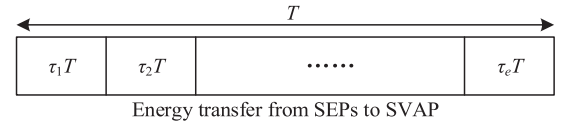


Fig. 4. Structure of the time frame for energy transfer.

receives RF energy through the Wi-Fi antenna. Therefore, during each time frame  $T$ , the data from a cell-edge device to its associated SVAP can be sent anytime, but a SVAP (e.g.,  $v$ ) can only receive energy from its  $|R_v|$  SEPs in a TDMA mode. The timing structure diagram for energy transfer is shown in Fig. 4, where  $0 < \tau_e < 1 \forall e \in \{1, 2, \dots, |R_v|\}$ , and  $\sum_{e \in \{1, 2, \dots, |R_v|\}} \tau_e = 1$ .

## IV. SCHEME STATEMENT

As mentioned above, to motivate the set of SEPs and the set of SVAPs to provide recharging service and data relaying service, respectively, the SBS must pay them spectrum as a reward. Therefore, the SBS offers a desired partition of the resource block obtained by a cell-edge device, where the free part of the resource block is divided into two parts and then allocated to the set of SEPs and the set of SVAPs, respectively. All the SEPs compete for their own share, and then, all the SVAPs compete for their own share on the basis of the results of the SEPs' competition results.

Because of these conditions, the Stackelberg game model [22] is applicable in our incentive architecture, where the SBS acts as the leader while the set of SEPs and the set of SVAPs act as the followers. During the decision process for each group of the followers, noncooperative game is used to model the resource competition among them. Before going into the details of the incentive architecture, we need to introduce the wireless signal propagation models used in this article.

### A. Wireless Signal Propagation Model

When a wireless node  $i$  works in the wireless power transfer mode, the power harvested by a wireless node  $j$  can be calculated as follows:

$$p_{i,j}^r = \eta_{i,j} p_{i,j}^t g_{i,j} \quad (1)$$

where  $p_{i,j}^t$  and  $p_{i,j}^r$  denote the transmission power at source  $i$  and the harvested power at receiver  $j$ , respectively, while  $\eta_{i,j}$  and  $g_{i,j}$  denote the efficiency coefficient of power conversion and the channel power gain between source  $i$  and receiver  $j$ , respectively. According to the wireless signal propagation models in [6],  $g_{i,j}$  can be estimated by the following formula:

$$\begin{cases} g_{i,j} = \frac{G_t G_r \lambda^2}{(4\pi d_{i,j})^2 L} & d_{i,j} < d_{\text{crossover}} \quad (\text{a}) \\ g_{i,j} = \frac{G_t G_r h_t^2 h_r^2}{d_{i,j}^4} & d_{i,j} \geq d_{\text{crossover}} \quad (\text{b}) \\ d_{\text{crossover}} = \frac{4\pi\sqrt{L}h_t h_r}{\lambda} & (\text{c}) \end{cases} \quad (2)$$

where  $G_t$  and  $G_r$  are the transmitting and receiving antenna gains, respectively;  $h_t$  and  $h_r$  are the transmitting and receiving antenna heights, respectively;  $\lambda$  is the wavelength of the signal carrier and  $L$  is the system loss coefficient which is not related

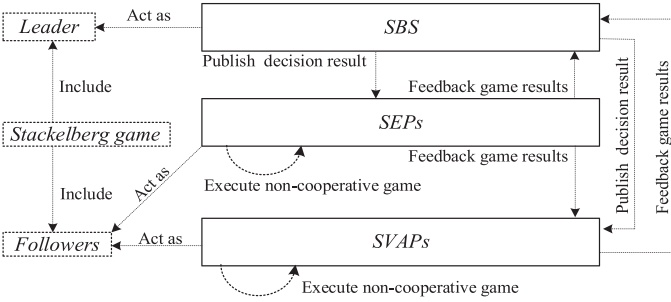


Fig. 5. Incentive architecture with dynamic charging.

to propagation, while  $d_{i,j}$  is the distance between source  $i$  and receiver  $j$ ; and  $d_{\text{crossover}}$  denotes the crossover distance.

When a wireless node  $i$  works in the wireless information transmission mode, the data rate  $b_{i,j}$  decoded by a wireless node  $j$  can be calculated as follows:

$$b_{i,j} = W \log_2 \left( 1 + \frac{p_{i,j}^t g_{i,j}}{\sigma^2 + F_j} \right) \quad (3)$$

where  $\sigma^2$  represents the noise power around the wireless node  $j$ , and  $F_j$  is the interference power perceived by the wireless node  $j$ , which is estimated by

$$F_j = \sum_{k \in I_j} g_{k,j} p_k \quad (4)$$

where  $g_{k,j}$  denotes the channel power gain from the interfering source  $k$  to the interfered node  $j$ ;  $p_k$  is the transmission power of the interfering source  $k$ ; and  $I_j$  is the set of the interfering sources of the node  $j$ .

### B. Incentive Architecture

Utilizing the Stackelberg game theory along with the noncooperative game theory, we design an incentive architecture to promote cooperation to improve the SE of cell-edge devices, which is shown in Fig. 5.

When the SBS allocates a resource block  $W$  to a cell-edge device, it wants this resource to be fully utilized. A portion of  $W$  should be set aside for the SBS for unified scheduling to motivate a SVAP to relay the data coming from the cell-edge device and to activate a set of SEPs to recharge this SVAP.

When a set of SEPs gets the frequency band share (i.e.,  $\xi_e W$ ) from the SBS, each of them will determine its recharging power based on a noncooperative game model. In addition, when a set of SVAPs gets the frequency band share (i.e.,  $|S_s| \xi_v W$ ) from the SBS, each of them will determine its relaying power based on a noncooperative game model. In a noncooperative game, each game player aims to maximize its data rate by acquiring the desired frequency band proportion.

If a greater share of  $W$  is allocated to the SVAP and the SEPs, it may not be conducive to the application experience of the cell-edge device as there is inadequate sharing of  $W$  for the cell-edge device's own use. On the contrary, the SVAP and the SEPs will have less incentive to offer the relaying service and the recharging service.

Therefore, to describe how the decision in the SBS is affected by the noncooperative game results of SEPs and SVAPs, we model their interaction as a two-level Stackelberg game. In the leading level, the SBS acts as the leader and announces the division proportion of  $W$  to ensure its maximum utility. In the following level, given the division ratio of  $W$ , the SEPs act as the followers and determine their charging powers according to their respective utility function. Then, given the division ratio of  $W$  and the recharging powers from the SEPs, the SVAPs act as the followers and decide their powers used in relaying data from a cell-edge device to the SBS according to their respective utility function.

### C. Utility of SEPs

For any SEP (e.g.,  $e$ ), when its maximum transmission power is set to  $p_e^{\max}$ , the power used in transferring energy from  $e$  to  $v \in S_s$  (i.e.,  $p_{e,v}^t$ ) and that used in transferring data from  $e$  to  $s$  (i.e.,  $p_{e,s}^t$ ) must satisfy the following relation:

$$p_e^{\max} \geq p_{e,v}^t + p_{e,s}^t. \quad (5)$$

Typically, the SEP  $e$  should use the greater value of  $p_{e,v}^t$  to transfer energy to the SVAP to exchange more of the spectrum for access to the cellular network. However, it has to adopt the greater value of  $p_{e,s}^t$  to send its own data such that the obtained spectrum is fully utilized. Therefore, the SEP  $e$  has to determine the optimal transmission power splitting ratio under the constraint of  $p_e^{\max}$ . When it employs  $p_e^{\max}$  and its battery energy reserve is  $E_e$ , its continuous transmission time (i.e.,  $T_e^{\max}$ ) can be estimated by the following formula:

$$T_e^{\max} = \frac{E_e}{p_e^{\max}}. \quad (6)$$

During  $T_e^{\max}$ , the utility function of the SEP  $e$  is described as follows:

$$\begin{cases} \mu_e(P_e) = T_e^{\max} \varphi_{e,s} \xi_e W \log_2 \left( 1 + \frac{(p_e^{\max} - p_{e,v}^t) g_{e,s}}{\sigma^2 + F_s} \right) \\ \varphi_{e,s} = \frac{\log_2 \left( 1 + \frac{\eta_{e,v} p_{e,v}^t g_{e,v} g_{v,s}}{\sigma^2 + F_s} \right)}{\Phi_e + \sum_{e' \in R_v} \log_2 \left( 1 + \frac{\eta_{e',v} p_{e',v}^t g_{e',v} g_{v,s}}{\sigma^2 + F_s} \right)} \\ P_e = \{p_{e',s}^t | \forall e' \in R_v\} \end{cases} \quad (7)$$

where  $\Phi_e$  is regarded as the contribution from a fictitious selfless node and usually set to a constant (e.g.,  $10^{-6}$ ), where its goal is to prevent game participants from colluding to cheat;  $\varphi_{e,s}$  represents the contribution ratio of the SEP  $e$  recharging the SVAP  $v$ .

### D. Utility of SVAPs

For any SVAP (e.g.,  $v$ ), we can adopt the following formula to estimate its harvesting energy from the  $|R_v|$  SEPs:

$$e_v = \sum_{e \in R_v} T_e^{\max} \eta_{e,v} p_{e,v}^t g_{e,v}. \quad (8)$$

Additionally, when the SVAP  $v$  sets its maximum transmission power to  $p_v^{\max}$ , the power used in relaying data from a cell-edge device to the SBS  $s$  (i.e.,  $p_{v,s}^t$ ) and that used in transmitting

its own data to the SBS  $s$  (i.e.,  $p_{u,s}^t$ ) must meet the following relation:

$$p_v^{\max} \geq p_{v,s}^t + p_{u,s}^t. \quad (9)$$

Usually, the SVAP  $v$  should adopt the greater value of  $p_{v,s}^t$  to relay data to the SBS  $s$  such that more of the spectrum for access to the cellular network can be secured. However, it has to employ the greater value of  $p_{u,s}^t$  to send its own data in order to fully utilize the obtained spectrum.

Therefore, the SVAP  $v$  has to determine the optimal transmission power splitting ratio under the constraint of  $p_v^{\max}$ . When it employs  $p_v^{\max}$ , and its battery energy reserve and harvested energy from the SEPs are  $E_v$  and  $e_v$ , respectively, its continuous transmission time (i.e.,  $T_v^{\max}$ ) can be estimated by the following formula:

$$T_v^{\max} = \frac{E_v + e_v}{p_v^{\max}}. \quad (10)$$

During  $T_v^{\max}$ , the utility function of the SVAP  $v$  is described as follows:

$$\begin{cases} \mu_v(P_v) = T_v^{\max} \varphi_{v,s} |S_s| \xi_v W \log_2 \left( 1 + \frac{(p_v^{\max} - p_{v,s}^t) g_{v,s}}{\sigma^2 + F_s} \right) \\ \varphi_{v,s} = \frac{\log_2 \left( 1 + \frac{p_{v,s}^t g_{v,s}}{\sigma^2 + F_s} \right)}{\Phi_v + \sum_{v' \in S_s} \log_2 \left( 1 + \frac{p_{v',s}^t g_{v',s}}{\sigma^2 + F_s} \right)} \\ P_v = \{p_{v',s}^t | \forall v' \in S_s\} \end{cases} \quad (11)$$

where  $\Phi_v$  is regarded as the contribution from a fictitious selfless node and usually set to a constant (e.g., 2), where, like  $\Phi_e$ , its aim is to prevent game participants from colluding to cheat;  $\varphi_{v,s}$  represents the contribution ratio of the SVAP  $v$  relaying the data of the cell-edge device. In addition, we only consider that a SVAP serves an associated cell-edge device in this article, so the number of cell-edge devices is the same as the number of SVAPs.

### E. Utility of SBS

Since SE is one focus of the SBS  $s$ , its utility can be calculated by

$$\sum_{\substack{\forall v \in S_s \\ \exists u \in U_v}} \left( \begin{aligned} \mu_s(\xi_e, \xi_v) &= \psi_e \psi_v W T_v^{\max} \\ &\left( (1 - \xi_e - \xi_v) \log_2 \left( 1 + \frac{p_{v,s}^t g_{v,s}}{\sigma^2 + F_s} \right) \right. \\ &\quad \left. - \log_2 \left( 1 + \frac{p_{u,s}^{\max} g_{u,s}}{\sigma^2 + F_s} \right) \right) \end{aligned} \right) \quad (12)$$

where the utility  $\mu_s(\xi_e, \xi_v)$  refers to the benefits brought by all the cell-edge devices that transmit data to the SBS via SVAPs when compared with those brought by the same cell-edge devices that directly send data to the SBS;  $u$  denotes a cell-edge device associated with a SVAP;  $\psi_e$  and  $\psi_v$  are the incentive coefficients for the SEPs and SVAPs, respectively, which means that the SEPs and SVAPs will have more incentive to offer the relaying service and recharging service if the two coefficients are larger. When the SEPs and SVAPs can get more free bandwidth resources, the two coefficients are relatively larger. Otherwise, they may be relatively smaller.  $\psi_e$  and  $\psi_v$  are estimated by the

following formula:

$$\begin{cases} \psi_e = \frac{\mu_e^t}{\mu_e^{\max}} & \text{(a)} \\ \psi_v = \frac{\mu_v^t}{\mu_v^{\max}} & \text{(b)} \end{cases} \quad (13)$$

where  $\mu_e^t$  is the total data of access to the SBS for the SEPs while  $\mu_v^t$  is the total data of access to the SBS for the SVAPs. They are estimated by the following formula:

$$\begin{cases} \mu_e^t = \sum_{v \in S_s} \sum_{e \in R_v} \left( T_e^{\max} \varphi_{e,s} \xi_e W \log_2 \left( 1 + \frac{(p_e^{\max} - p_{e,v}^t) g_{e,s}}{\sigma^2 + F_s} \right) \right) & \text{(a)} \\ \mu_v^t = \sum_{v \in S_s} \left( T_v^{\max} \varphi_{v,s} \xi_v |S_s| W \log_2 \left( 1 + \frac{(p_v^{\max} - p_{v,s}^t) g_{v,s}}{\sigma^2 + F_s} \right) \right) & \text{(b)} \end{cases} \quad (14)$$

In (13),  $\mu_e^{\max}$  and  $\mu_v^{\max}$  are the ideal maximum values of  $\mu_e^t$  and  $\mu_v^t$ , respectively. Let  $\xi_e = 1$ , the value of  $\mu_e^{\max}$  can be obtained by formula (14a). In addition, let  $\xi_v = 1$ , the value of  $\mu_v^{\max}$  can be obtained by formula (14b).

## V. ANALYSIS OF THE PROPOSED SCHEME

In the above section, we put forward the incentive architecture based on Stackelberg game, which models the interaction between the SBS and the two sets of UE (i.e., the set of SEPs and the set of SVAPs). In the section, we use the backward induction method to analyze the proposed two-level Stackelberg game. First, for the following level, there are the two decision processes that we need to analyze, which are the decision process of the SEPs and the decision process of the SVAPs. Each SVAP only has one-way dependence on its associated SEPs and there is no game relationship between them. Therefore, given the leader's action strategy, the optimal decisions of the SEPs on the recharging powers need to be first analyzed and solved, and then, the optimal decisions of the SVAPs on the relaying powers are analyzed and solved based on the recharging powers of the SEPs. Then, in the leading level, based on the decision results of the SEPs and SVAPs, the optimal decision of the SBS on the division proportion of  $W$  is analyzed and solved.

### A. Optimal Recharging Powers for SEPs

A noncooperative scenario is considered in this subsection since all the SEPs are rational and self-interested. That is, each of them only wants to minimize its recharging power and maximize its transmitting power. Therefore, in the proposed noncooperative game for the SEPs, each SEP in  $R_v$  is the game player, and it determines the recharging power and data transfer power under the constraint of its maximum transmission power and independently decides its game action strategy based on its game utility value (i.e., the data rate).

It is worth noting that each player's strategy (e.g.,  $p_{e,v}^t$  of the SEP  $e$ ) only depends on the strategies of the other game players (i.e.,  $P_{-e} = \{p_{e',v}^t | \forall e' \in R_v \text{ and } e' \neq e\}$ ). Thus, when the strategies of the other game players  $P_{-e}$  are given, the solution to the following optimization problem (15) will be the best response strategy for the SEP  $e$ . That is, the SEP  $e$  needs to

find the optimal transmission power  $p_{e,v}^t$  to offer to the SVAP  $v$  to maximize its individual earnings, which can be acquired by solving the following optimization problem:

$$\max_{\{p_{e,v}^t, P_{-e}\}} \left\{ T_e^{\max} \varphi_{e,s} \xi_e W \log_2 \left( 1 + \frac{(p_e^{\max} - p_{e,v}^t) g_{e,s}}{\sigma^2 + F_s} \right) \right\}. \quad (15)$$

*Theorem 1:* There exists an optimal response strategy for the optimization problem (15).

*Proof:* See Appendix A for the proof.

Based on the proof of Theorem 1, let  $\frac{\partial \mu_e(P_e)}{\partial p_{e,v}^t} = 0$ , and then, the optimal response strategy  $p_{e,v}^{t*}$  of the SEP  $e$  can be solved in theory. In fact, “ $\frac{\partial \mu_e(P_e)}{\partial p_{e,v}^t} = 0$ ” is a transcendental equation, and we cannot directly solve its optimal solution. Therefore, in the following, we will solve it by designing an algorithm based on the idea of binary search.

### B. Optimal Relaying Powers for SVAPs

Like the SEPs, the SVAPs are all rational and self-interested, and they only want to minimize their relaying powers and maximize their transmitting powers. Therefore, in the proposed noncooperative game for the SVAPs, the  $|S_s|$  SVAPs are the game players, and they independently decide their game actions based on their game utility values (i.e., the data rate for each SVAP), where each SVAP determines the relaying power and transmitting power under the constraint of its maximum transmission power.

It is worth noting that each player’s strategy (e.g.,  $p_{v,s}^t$  of the SVAP  $v$ ) only depends on the strategies of the other players (i.e.,  $P_{-v} = \{p_{v',s}^t | \forall v' \in S_s \text{ and } v' \neq v\}$ ). Thus, when the strategies of the other players  $P_{-v}$  are given, the solution to the following optimization problem (16) will be the best response strategy for the SVAP  $v$ . That is, the SVAP  $v$  needs to find the optimal transmission power  $p_{v,s}^t$  to offer the data forwarding service for its associated cell-edge device to maximize its individual earnings, which can be achieved by solving the following optimization problem:

$$\max_{\{p_{v,s}^t, P_{-v}\}} \left\{ T_v^{\max} \varphi_{v,s} |S_s| \xi_v W \log_2 \left( 1 + \frac{(p_v^{\max} - p_{v,s}^t) g_{v,s}}{\sigma^2 + F_s} \right) \right\}. \quad (16)$$

*Theorem 2:* There exists an optimal response strategy for the optimization problem (16).

*Proof:* The proof of Theorem 2 is similar to that of Theorem 1.

Based on the proof of Theorem 2, let  $\frac{\partial \mu_v(P_v)}{\partial p_{v,s}^t} = 0$ , the optimal response strategy  $p_{v,s}^{t*}$  of the SVAP  $v$  can be solved in theory. In fact, “ $\frac{\partial \mu_v(P_v)}{\partial p_{v,s}^t} = 0$ ” is a transcendental equation, and we cannot directly solve its optimal solution. Therefore, in the following, we will solve it by designing an algorithm based on the idea of binary search.

### C. Optimal Division Proportion of W for SBS

So far, we have got the optimal recharging powers and the optimal relaying powers in the following level. Then, we can obtain the best response strategy of the SBS  $s$  by solving the following optimization problem in the leading level:

$$\max_{\{\xi_e, \xi_v\}} \left\{ \psi_e \psi_v W T_v^{\max} \sum_{\substack{\forall v \in S_s \\ \exists u \in U_v}} \left( (1 - \xi_e - \xi_v) \log_2 \left( 1 + \frac{p_{v,s}^t g_{v,s}}{\sigma^2 + F_s} \right) - \log_2 \left( 1 + \frac{p_u^{\max} g_{u,s}}{\sigma^2 + F_s} \right) \right) \right\}. \quad (17)$$

*Theorem 3:* There exists a suboptimal response strategy for the optimization problem (17).

*Proof:* See Appendix B for the proof.

Based on the proof of Theorem 3, let  $\frac{\partial \mu_s(\xi_e, \xi_v)}{\partial \xi_v} = 0$ , the suboptimal response strategy  $\xi_v^{*}$  can be solved in theory. Also, let  $\frac{\partial \mu_s(\xi_e, \xi_v^{*})}{\partial \xi_e} = 0$ , the suboptimal response strategy  $\xi_e^{*}$  can be solved in theory. In fact, “ $\frac{\partial \mu_s(\xi_e, \xi_v)}{\partial \xi_v} = 0$ ” and “ $\frac{\partial \mu_s(\xi_e, \xi_v^{*})}{\partial \xi_e} = 0$ ” belong to a transcendental equation, respectively, and we cannot directly solve for the above suboptimal solutions. Therefore, in the following, we will solve them by designing an algorithm based on the idea of binary search.

### D. Theoretical Analysis for Noncooperative Game

In this subsection, we will prove the convergence of interactive processes based on the utility functions of (7) and (11). To this end, the potential game [23] is first introduced, which can guarantee the existence of at least a Nash equilibrium (NE) point. The formalized potential game is denoted as  $\Theta = \langle \Omega, A, \mu \rangle$  [24], where  $\Omega = \{1, 2, \dots, n\}$  represents a set of game players;  $A = \prod_{i=1}^n A_i$  represents the space of all action vectors, where  $A_i$  is the set of the  $i$ th game player’s actions; and  $\mu = \langle \mu_1, \dots, \mu_i, \dots, \mu_n \rangle$  denotes a utility function vector, where  $\mu_i$  is the utility for the  $i$ th game player. More specifically,  $\Omega$  is treated as either a set of SEPs or a set of SVAPs. When  $\Omega$  is actually a set of SEPs,  $\mu_i$  is the utility for the  $i$ th SEP, which is measured by (7). When  $\Omega$  is actually a set of SVAPs,  $\mu_i$  is the utility for the  $i$ th SVAP, which is measured by (11).

$a_i (a_i \in A_i)$  is a component in vector  $a (a \in A)$ . In addition,  $a = \langle a_i, a_{-i} \rangle$  denotes an action profile, where  $a_i$  is the game player  $i$ ’s action, and  $a_{-i}$  represents the actions of the other  $n-1$  game players. Similarly,  $A_{-i} = \prod_{j \neq i} A_j$  is the set of action strategy profiles for all game players except for the game player  $i$ . According to [24], the formal definition for NE is given as follows.

*Definition 1:* For  $\forall i \in \Omega$  and  $\forall a_i \in A_i$ , if  $\mu_i(a^*) \geq \mu_i(a_i, a_{-i}^*)$ , the action profile  $a^* = (a_i^*, a_{-i}^*)$  is an NE.

According to [24], the relationship between the ordinal potential game (OPG) and the ordinal potential function (OPF) is defined as follows.

*Definition 2:* If there is a function  $F : A \rightarrow \mathbb{R}$  such that  $F(a_i, a_{-i}) - F(b_i, a_{-i}) > 0 \Leftrightarrow \mu_i(a_i, a_{-i}) - \mu_i(b_i, a_{-i}) > 0$

under the conditions that  $\forall i \in \Omega, \forall a_{-i} \in A_{-i}$ , and  $\forall a_i, b_i \in A_i$ , the game  $\Theta = \langle \Omega, A, \mu \rangle$  is an OPG and  $F$  is an OPF of  $\Theta$ .

If an OPG (e.g.,  $\Theta = \langle \Omega, A, \mu \rangle$ ) can optimize the corresponding OPF (e.g.,  $F$ ), there exists a NE [23], [24]. Therefore, a subset of NEs in a potential game consists of a set of potential maximizers. If a set of potential functions of a potential game can be found, some NEs of the potential game can be found by solving for the potential maximizers.

The game  $\Theta = \langle \Omega, A, \mu \rangle$ , where  $\Omega$  is a set of SEPs (i.e.,  $\Omega = R_v$ ) and the utility function of each SEP is given by (7), is a potential game, which is given as follows.

*Theorem 4:* The game  $\Theta = \langle \Omega, A, \mu \rangle$ , where the individual utilities are given by (7), is an OPG. An OPF is given as follows:

$$F(P_e) = \sum_{e=1}^{|R_v|} \mu_e(P_e). \quad (18)$$

*Proof:* See Appendix C for the proof.

The game  $\Theta = \langle \Omega, A, \mu \rangle$ , where  $\Omega$  is a set of SVAPs (i.e.,  $\Omega = S_s$ ) and the utility function of each SVAP is given by (11), is a potential game, which is given as follows.

*Theorem 5:* The game  $\Theta = \langle \Omega, A, \mu \rangle$ , where the individual utilities are given by (11), is an OPG. An OPF is given as follows:

$$F(P_v) = \sum_{v=1}^{|S_s|} \mu_v(P_v). \quad (19)$$

The proof of Theorem 5 is similar to that of Theorem 4, so it is not elaborated. According to Theorems 4 and 5, the utility functions described in (7) and (11) have the characteristics of the potential game, which ensures that there is at least one NE.

## VI. ALGORITHM DESIGN FOR OUR SCHEME

Although we have proved the existence of the optimal partition of the resource block  $W$ , it is difficult to obtain this value directly due to the existence of transcendental equations. Inspired by [25], we propose a set of algorithms to approach this objective, which is described as follows.

First, the SBS offers an initial partition ratio of  $W$  to the SEPs and SVAPs. Then, each SEP determines the recharging power that it adopts to recharge its associated SVAP by running Algorithm 1. Next, each SVAP determines the transmission power that it adopts to relay data from its associating cell-edge device to the SBS by running Algorithm 2. Finally, the SBS updates its partition ratio by running Algorithm 3. Steps 2–4 are repeated until the partition ratio value converges.

The above three algorithms all invoke the proposed algorithm based on the idea of binary search, and the corresponding pseudocode is shown in Algorithm 4.

In Algorithm 4, the utility function  $\mu(x)$  is explained as

$$\mu(x) = \begin{cases} \mu_e(x), & \text{SEP - level game} \\ \mu_v(x), & \text{SVAP - level game} \\ \mu_s(\xi_e, x), & \text{SBS - level game, let } \xi_e \text{ be a constant} \\ \mu_s(x, \xi_v), & \text{SBS - level game, let } \xi_v \text{ be a constant} \end{cases} \quad (20)$$

Although the precise global optimal solution cannot be obtained by using the above algorithms, we can always find an

---

### Algorithm 1: SEP-Level Game.

---

Run at any SEP  $e \in R_v$

Input:  $\varepsilon$

Output:  $(p_{e,v}^t, p_{e,s}^t)$

---

```

1: If receive  $\xi_e, \xi_v, \varphi_{v,s}$ , and  $\varphi_{e,s}$  from the SBS  $s$  then
2:    $\min = 0$ ;  $\max = p_e^{\max}$ 
3:    $p_{e,v}^t = \text{BinarySearch}(\min, \max)$ 
4:    $p_{e,s}^t = p_e^{\max} - p_{e,v}^t$ 
5:   send  $(p_{e,v}^t, p_{e,s}^t)$  to the SBS  $s$ 
6:   While (true) do
7:     If receive  $\varphi_{e,s}$  from the SBS  $s$  then
8:        $p_{e,v}^t = \text{BinarySearch}(\min, \max)$ 
9:        $p_{e,s}^t = p_e^{\max} - p_{e,v}^t$ 
10:      send  $(p_{e,v}^t, p_{e,s}^t)$  to the SBS  $s$ 
11:     End if
12:     If receive “end” from the SBS  $s$  then
13:       send  $(p_{e,v}^t, p_{e,s}^t)$  to the SVAP  $v$  and return
14:     End if
15:   End while
16: End if

```

---



---

### Algorithm 2: SVAP-Level Game.

---

Run at any SVAP  $v \in S_s$

Input:  $\varepsilon$

Output:  $(p_{v,s}^t, p_{u,s}^t)$

---

```

1: If receive  $\{(p_{e,v}^t, p_{e,s}^t) | e \in R_v\}$  from all the SEPs in
    $R_v$  and  $\xi_v, \varphi_{v,s}$  from the SBS  $s$  then
2:    $\min = 0$ ;  $\max = p_v^{\max}$ 
3:    $p_{v,s}^t = \text{BinarySearch}(\min, \max)$ 
4:    $p_{u,s}^t = p_v^{\max} - p_{v,s}^t$ 
5:   send  $(p_{v,s}^t, p_{u,s}^t)$  to the SBS  $s$ 
6:   While (true) do
7:     If receive  $\varphi_{v,s}$  from the SBS  $s$  then
8:        $p_{v,s}^t = \text{BinarySearch}(\min, \max)$ 
9:        $p_{u,s}^t = p_v^{\max} - p_{v,s}^t$ 
10:      send  $(p_{v,s}^t, p_{u,s}^t)$  to the SBS  $s$ 
11:     End if
12:     If receive “end” from the SBS  $s$  then return End if
13:   End while
14: End if

```

---

approximate solution that meets the specific application requirements by controlling the value of the parameter  $\varepsilon$ . In particular, if the parameter  $\varepsilon$  is small enough, the approximate solution obtained by the algorithms is close enough to the global optimal solution at the expense of more running overhead. In this article, the parameter  $\varepsilon$  in the four algorithms is set to a moderate value (e.g., 0.1%). Moreover, some parameter variables (e.g.,  $\xi_e, \xi_v, \varphi_{e,s}, \varphi_{v,s}, p_{e,v}^t, p_{e,s}^t, p_{v,s}^t, p_{u,s}^t$ ) in the algorithms need to be given initial values. In general, due to the convergence of the algorithms, the expected results can be achieved as long as the initial values are within the range of values of these parameter

**Algorithm 3: SBS-Level Game.**


---

Run at the SBS  $s$   
Input:  $\varepsilon$   
Output:  $\xi_e, \xi_v$

---

- 1: initialize  $\xi_e$  and  $\xi_v$  as 0.2, respectively
- 2: initialize  $c_e, c_v$  and flag as 0, respectively
- 3: **For** each SEP  $e$  **do**
- 4:    $p_{e,v}^t = \frac{p_e^{\max}}{2}$ ;  $p_{e,s}^t = p_e^{\max} - p_{e,v}^t$ ;  $c_e ++$
- 5: **End for**
- 6: **For** each SVAP  $v$  **do**
- 7:    $p_{v,s}^t = \frac{p_v^{\max}}{2}$ ;  $p_{v,s}^t = p_v^{\max} - p_{v,s}^t$ ;  $c_v ++$
- 8: **End for**
- 9:  $\mu = \mu_s(\xi_e, \xi_v)$
- 10: initialize  $\varphi_{e,s}$  as  $\frac{c_v}{c_e}$
- 11: initialize  $\varphi_{v,s}$  as  $\frac{1}{c_v}$
- 12: broadcast  $\xi_e, \xi_v, \varphi_{v,s}$ , and  $\varphi_{e,s}$  to all the SEPs and SVAPs
- 13: **While** (*true*) **do**
- 14:   **If** receive the updated  $(p_{e,v}^t, p_{e,s}^t)$  from any SEP  $e$  **then**
- 15:     replace the old value of  $(p_{e,v}^t, p_{e,s}^t)$  with its new value
- 16:   **Else if** receive the old  $(p_{e,v}^t, p_{e,s}^t)$  from any SEP  $e$  **then**
- 17:     record the cumulative number of SEPs sending old values
- 18:   **End if**
- 19:   **If** all the SEPs report  $(p_{e,v}^t, p_{e,s}^t)$  and there is at least a new value **then**
- 20:     **For** each SEP  $e$  **do** compute  $\varphi_{e,s}$  and send it to  $e$
- 21:     **End for**
- 22:   **End if**
- 23:   **If** all the SEPs report the old  $(p_{e,v}^t, p_{e,s}^t)$  **then**
- 24:     broadcast the packet including the “end” to all the SEPs
- 25:   **End if**
- 26:   **If** receive the updated  $(p_{v,s}^t, p_{u,s}^t)$  from any SVAP  $v$  **then**
- 27:     replace the old value of  $(p_{v,s}^t, p_{u,s}^t)$  with its new value
- 28:   **Else if** receive the old  $(p_{v,s}^t, p_{u,s}^t)$  from any SVAP  $v$  **then**
- 29:     record the cumulative number of SVAPs sending old values
- 30:   **End if**
- 31:   **If** all the SVAPs report  $(p_{v,s}^t, p_{u,s}^t)$  and there is at least a new value **then**
- 32:     **For** each SVAP  $v$  **do** compute  $\varphi_{v,s}$ ; send it to  $v$
- 33:     **End for**
- 34:   **End if**
- 35:   **If** all the SVAPs report the old  $(p_{v,s}^t, p_{u,s}^t)$  **then**
- 36:     broadcast the packet including the “end” to all the SVAPs
- 37:   **End if**
- 38:    $\min = 0$ ;  $\max = 1$

---

- 36:    $\xi'_v = \text{BinarySearch}(\min, \max)$ ;  $\xi_v = \xi'_v$  //Let  $\xi_e$  take the current value and optimize  $\xi_v$
- 37:    $\xi'_e = \text{BinarySearch}(\min, \max)$ ;  $\xi_e = \xi'_e$  //Let  $\xi_v$  take the current value and optimize  $\xi_e$
- 38:   **If**  $\mu_s(\xi_e, \xi_v) > \mu$  **then** go to 9 **Else** break **End if**
- 39: **End if**
- 40: **End while**

---

**Algorithm 4: BinarySearch(min,max).**


---

Input:  $\varepsilon$   
Output:  $p$

---

- 1: **While** ( $|\max - \min| > \varepsilon$ ) **do**
- 2:    $p = \frac{\min + \max}{2}$
- 3:   **If**  $\mu(p - \varepsilon) > \mu(p)$  **then**  $\max = p$  **Else**  $\min = p$  **End if**
- 4: **End while**
- 5: return  $p$

---

variables. Reasonable initial values can make the algorithms converge faster. If you do not know what reasonable initial values are, you can simply take the average of the range of values.

## VII. PERFORMANCE EVALUATION

### A. Simulation Parameter Settings

In our simulations, the microcell has a radius of 200 m, where the SBS is located at its center, and the UE are randomly distributed in its coverage. As shown in Fig. 1, the eight reference points are uniformly distributed on the circle whose radius  $R_{th}$  has a value of 60 m. Each SEP or SVAP is selected from the UE according to the conditions described in Section III-A.

The UE that are associated with each SVAP are basically located near the edge of the microcell because such UE need the help of VAPs more. Without loss of generality, we only focus on the case that each SVAP only serves a cell-edge device (i.e., a UE associated with it). Unless otherwise stated, the simulation parameters are as listed in Table 1.

### B. Simulation Results and Analysis

First, three simulations are shown in Fig. 6, where we mainly evaluate the average SE for cell-edge devices. Then, three other simulations are given in Fig. 7, where we evaluate the average SE for SEPs and SVAPs, respectively.

From Fig. 6(a), we can see that the impact of the UE density (i.e., the number of UE in a fixed region) on the SE of cell-edge devices is random. As the density of UE increases, the selected SVAP tends to be closer to the reference point, but it is not necessarily closer to the SBS. Moreover, the SVAP associated with the cell-edge device may change randomly as the node density changes. Thus, the average SE will change accordingly.

In addition, Fig. 6(a) clearly shows that SVAPs can indeed improve the average SE for cell-edge devices. This is mainly because the long-distance communication between a cell-edge device and the SBS is avoided with the help of a SVAP. Thanks to

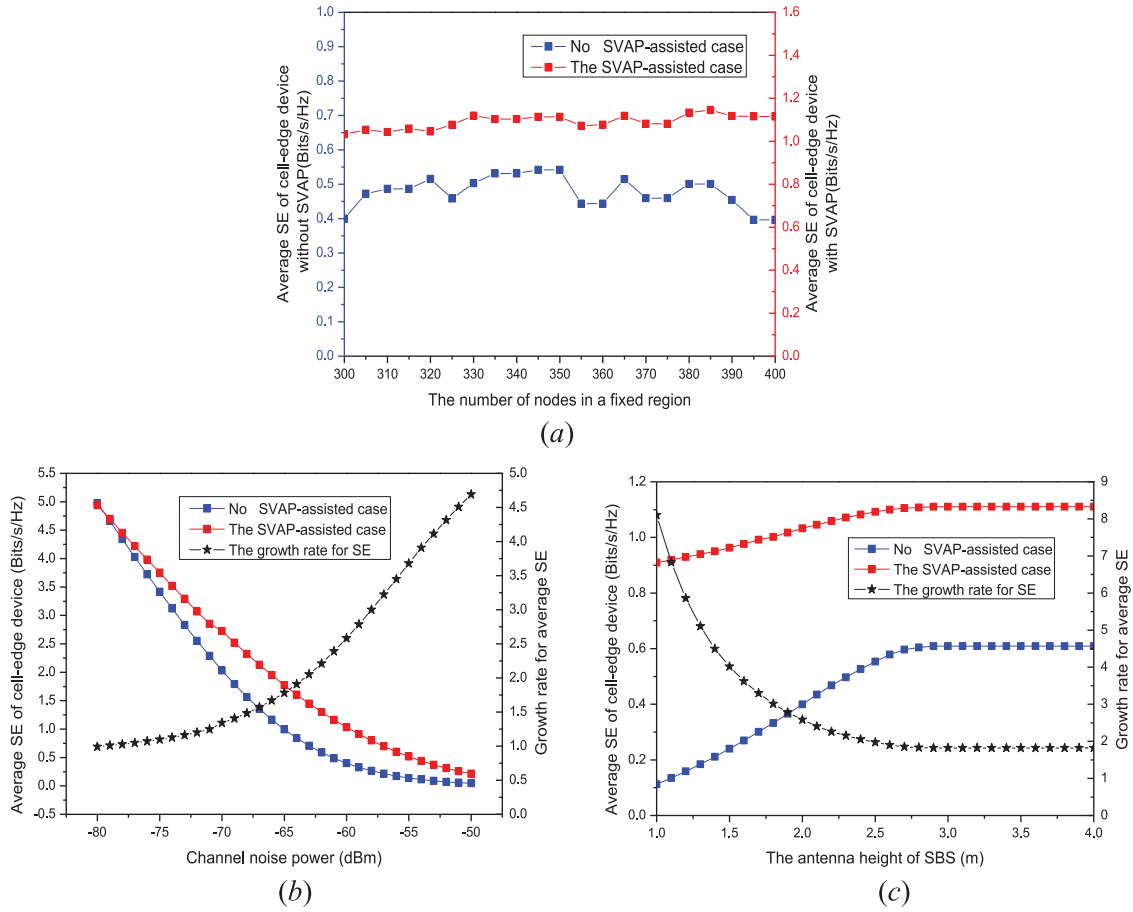


Fig. 6. Average SE and its growth rate for the cell-edge device. (a) Performance versus the number of UE in a fixed region. (b) Performance versus channel noise power. (c) Performance versus antenna height of SBS.

TABLE I  
SIMULATION PARAMETERS

Symbol	Description	Value
$p_u^{max}$	Maximum transmission power for UEs, including SEPs and SVAPs	26 dBm
$W$	Unit resource block (or bandwidth)	1 MHz
$G_t$	Transmitting antenna gain	1
$G_r$	Receiving antenna gain	1
$h_t$	Transmitting antenna height for UEs	1 m
$h_r$	Receiving antenna height	UEs: 1 m; SBS: 2 m
$\lambda$	Carrier signal wavelength for charging	0.1224 m
$L$	System loss factor for charging channel	1
$\eta_{i,j}$	Power conversion efficiency	0.56
$N$	The number for UEs	300
$\sigma^2$	Channel noise power	-60 dBm/MHz

the improved SE, a cell-edge device is able to provide a share of the spectrum resource as a rewarding resource without affecting its application experience.

As mentioned above, [5] is the closest to the work of this article. However, in [5], a cell-edge device does not need to contribute any spectrum resource. Therefore, with the help of a node similar to a SVAP, the SE of the cell-edge device can certainly be improved. However, such a scheme would require additional spectrum resources as rewarding resources, so the

SE of the entire system may not be improved. This is because the amount of such additional spectrum resources is not clearly defined and considered in system modeling.

As shown in Fig. 6(b), whether a cell-edge device is assisted by a SVAP or not, the average SE decreases with the increase of the channel noise power. However, the growth rate of SE increases with the increase of the channel noise power. This is because, with the increase of the channel noise power, a SVAP plays an increasingly significant role in improving the SE of a cell-edge device. When the channel noise power is relatively low, the SE of the cell-edge device without the help of a SVAP is even higher than that with the help of a SVAP. The main reason is that the cell-edge device can meet its traffic demand by directly communicating with the SBS under the low noise environment.

However, with the help of SVAP, it is necessary to allocate part of its resource block to the SVAP and some SEPs, which in turn may lead to smaller benefits under the low noise environment. Alternately, when the channel noise power is relatively high, a SVAP hardly has the ability to improve the SE of a cell-edge device. According to the Shannon theorem, it is easy to understand that in the case of limited transmission power, extremely high channel noise will make the channel capacity tend to zero, so SE also tends to zero. Therefore, the proposed scheme can

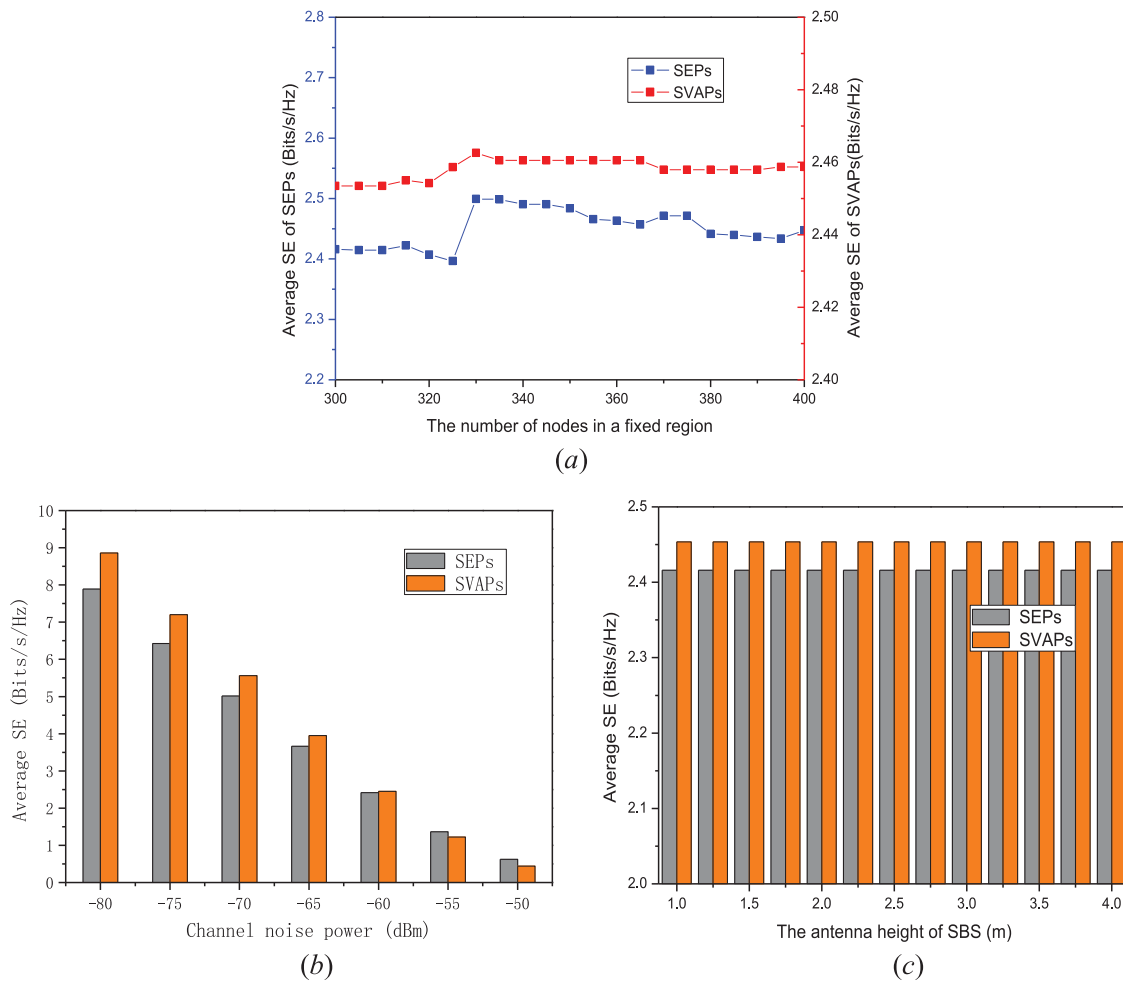


Fig. 7. Average SE for SEPs and SVAPs. (a) Performance versus the number of UE in a fixed region. (b) Performance versus channel noise power. (c) Performance versus antenna height of the SBS.

only work well in a certain range of channel noise powers. From Fig. 6(b), we can see that a SVAP plays a role in improving the SE of a cell-edge device when the channel noise power ranges from  $-75$  to  $-55$  dBm.

Fig. 6(c) reveals the performance in terms of the average SE and its growth rate under the change of the antenna height of the SBS. As the receiving antenna height of the SBS increases, the SE of the cell-edge device first shows an increasing trend and then, tends to be stable. This can be explained by formula (2), where the antenna height of the SBS affects the size of the crossover distance. That is, as the antenna height of the SBS increases, the crossover distance increases, and thus, the channel gain increases, which in turn leads to the increase of SE. However, when the SBS antenna is increased to a certain height, the communication distance between a cell-edge device and the SBS will be smaller than the crossover distance, and thus, the free space propagation model will be adopted. Because the free-space propagation model is not affected by the antenna height, it no longer affects the change of SE. Additionally, based on the same reason, we know why the growth rate of SE decreases with the increase of antenna height.

It can be seen from Fig. 7(a) that the impact of UE density on the average SE of the SEPs and SVAPs is random. As the node density increases, the selected SVAP will tend to be closer to the reference point, which in turn leads to the change of the associated SEPs. For a SVAP, it is closer to the reference point, but it is not necessarily closer to the SBS. Similarly, an SEP that is closer to the SVAP does not mean that it is closer to the SBS. Moreover, the change in the selected SEPs and SVAPs means a change in power allocation, which is also random.

From Fig. 7(b), we can observe that, with the increase of channel noise power, the average SE of the SEPs and SVAPs using free spectrum resources decreases. This can be explained by formulas (8) and (13), where the increase of channel noise power leads to the decrease of signal-to-noise ratio and thus, causes the overall SE to decrease.

From Fig. 7(c), we know that the antenna height has no effect on the average SE of the SEPs and SVAPs, which can be explained by formula (2). That is, the antenna height of the SBS affects the size of the crossover distance, where the crossover distance increases with the increase of the antenna height of the SBS. However, the distance between any SVAP and the SBS

is smaller than the crossover distance because  $R_{th}$  is valued at 60 m, even if the antenna takes the minimum height (e.g., 1). Moreover, the distance between an SEP and its associated SVAP is smaller than the crossover distance because the short distance is a key condition for a SVAP to select an SEP. Therefore, the channel gain calculation is independent of the antenna height, and thus, the antenna height has no effect on the average SE of the SEPs and SVAPs.

### C. Industrial Applications

In smart manufacturing plants, there are a large number of machine-type communication devices. They can usually maintain communication with business servers located in the cloud computing center via a cellular network. To maintain large concurrent connections between machine-type communication devices and a cellular base station, a large number of spectrum resources should be allocated to this base station for scheduling. Due to the good channel conditions of the sub-6 GHz frequency band, LTE/LTE-A for an M2M cellular network [26] is suitable to be built in an industrial park. However, there is a mismatch between the limited spectrum resources and the huge requirements for concurrent connections. Therefore, improving SE can alleviate this dilemma to some extent. Especially when a spectrum resource block is scheduled for the machine-type communication device on the edge of the M2M cellular network, our scheme can be extended to this scenario to improve SE.

## VIII. CONCLUSION

In this article, to improve the SE of cell-edge devices, we proposed a novel incentive architecture based on the dynamic RF recharging technology, which consists of the SBS, the SVAPs selected by the SBS, and the SEPs selected by each SVAP. In such an incentive architecture, the SBS aimed to identify the desired partition of each cell-edge device's resource block to maximize its utility, while the free part of this resource block will be rewarded to the SVAPs and the SEPs according to the contributions of relaying data and recharging service, respectively. The simulation results showed that each SVAP-assisted cell-edge device enhances its SE, and each SVAP and each SEP also receive the corresponding rewards. In addition, in real-life scenarios, there may be a time-varying characteristic for the selected SVAPs and SEPs. However, our scheme does not take this possibility into account, which is the direction of our future efforts.

### APPENDIX A PROOF OF THEOREM 1

$$\text{Let } \begin{cases} A = \varphi_{e,s} = \frac{\log_2 \left( 1 + \frac{\eta_{e,v} p_{e,v}^t g_{e,v} g_{v,s}}{\sigma^2 + F_s} \right)}{\phi_e + \sum_{e' \in R_v} \log_2 \left( 1 + \frac{\eta_{e',v} p_{e',v}^t g_{e',v} g_{v,s}}{\sigma^2 + F_s} \right)} \\ B = \log_2 \left( 1 + \frac{(p_e^{\max} - p_{e,v}^t) g_{e,s}}{\sigma^2 + F_s} \right) \end{cases} \quad (21)$$

Then, we have

$$\begin{cases} \frac{\mu_e(P_e)}{\partial(p_{e,v}^t)} = T_e^{\max} \xi_e W(AB)' = T_e^{\max} \xi_e W(A'B + AB') \\ \frac{\partial^2 \mu_e(P_e)}{\partial(p_{e,v}^t)^2} = (T_e^{\max} \xi_e W(A'B + AB'))' \\ = T_e^{\max} \xi_e W(A'B + 2A'B' + AB'') \end{cases} \quad (22)$$

In (21) and (22),  $A''B$ ,  $2A'B'$ , and  $AB''$  can be obtained by calculating the first and second derivatives of  $A$ , and the first and second derivatives of  $B$

$$\begin{aligned} A''B &= -\frac{1}{\ln 2} \cdot \frac{(\eta_{e,v} g_{e,v} g_{v,s})^2}{(\sigma^2 + F_s + \eta_{e,v} p_{e,v}^t g_{e,v} g_{v,s})^2} \\ &\quad \cdot \frac{\phi_e + \sum_{e' \in R_v \cap e' \neq e} \log_2 \left( 1 + \frac{\eta_{e',v} p_{e',v}^t g_{e',v} g_{v,s}}{\sigma^2 + F_s} \right)}{\left( \phi_e + \sum_{e' \in R_v} \log_2 \left( 1 + \frac{\eta_{e',v} p_{e',v}^t g_{e',v} g_{v,s}}{\sigma^2 + F_s} \right) \right)^2} \\ &\quad \cdot \left( \frac{2}{\ln 2} \cdot \frac{1}{\phi_e + \sum_{e' \in R_v} \log_2 \left( 1 + \frac{\eta_{e',v} p_{e',v}^t g_{e',v} g_{v,s}}{\sigma^2 + F_s} \right)} + 1 \right) \\ &\quad \cdot \log_2 \left( 1 + \frac{(p_e^{\max} - p_{e,v}^t) g_{e,s}}{\sigma^2 + F_s} \right) < 0 \\ 2A'B' &= -\frac{2}{(\ln 2)^2} \cdot \frac{\eta_{e,v} g_{e,v} g_{v,s}}{\sigma^2 + F_s + \eta_{e,v} p_{e,v}^t g_{e,v} g_{v,s}} \\ &\quad \cdot \frac{\phi_e + \sum_{e' \in R_v \cap e' \neq e} \log_2 \left( 1 + \frac{\eta_{e',v} p_{e',v}^t g_{e',v} g_{v,s}}{\sigma^2 + F_s} \right)}{\left( \phi_e + \sum_{e' \in R_v} \log_2 \left( 1 + \frac{\eta_{e',v} p_{e',v}^t g_{e',v} g_{v,s}}{\sigma^2 + F_s} \right) \right)^2} \\ &\quad \cdot \frac{g_{e,s}}{\sigma^2 + F_s + (p_e^{\max} - p_{e,v}^t) g_{e,s}} < 0 \\ AB'' &= -\frac{1}{\ln 2} \cdot \frac{\log_2 \left( 1 + \frac{\eta_{e,v} p_{e,v}^t g_{e,v} g_{v,s}}{\sigma^2 + F_s} \right)}{\phi_e + \sum_{e' \in R_v} \log_2 \left( 1 + \frac{\eta_{e',v} p_{e',v}^t g_{e',v} g_{v,s}}{\sigma^2 + F_s} \right)} \\ &\quad \cdot \frac{g_{e,s}^2}{(\sigma^2 + F_s + (p_e^{\max} - p_{e,v}^t) g_{e,s})^2} < 0. \end{aligned}$$

Therefore,  $\frac{\partial^2 \mu_e(P_e)}{\partial(p_{e,v}^t)^2} < 0$  so that for an arbitrary SEP  $v$ , its net utility function defined in (7) is a concave function with respect to  $p_{e,v}^t$ . In other words, the optimization problem (15) always has the optimal solution  $p_{e,v}^{t*}$ . That is the end of the proof.

### APPENDIX B PROOF OF THEOREM 3

Obviously, the optimization problem (17) can be formed as an equivalent binary function of  $\xi_e$  and  $\xi_v$ . However, it is difficult to solve the optimal solution  $\{\xi_e^*, \xi_v^*\}$ . According to [27], the bivariate optimization problem can be decomposed into the two univariate optimization problems, which can be solved separately to get the suboptimal solution  $\{\xi_e^*, \xi_v^*\}$ .

First, let  $\xi_e$  be a fixed value and demonstrate whether the net utility function defined in (12) is a concave function with respect to  $\xi_v$  or not.

Let

$$A = \psi_v = \frac{\sum_{v \in S_s} T_v^{\max} \varphi_{v,s} \xi_v |S_s| W \log_2 \left( 1 + \frac{(p_{v,s}^{\max} - p_{v,s}^t) g_{v,s}}{\sigma^2 + F_s} \right)}{\mu_v^{\max}}$$

$$B = \sum_{\substack{\forall v \in S_s \\ \exists u \in U_v}} \left( (1 - \xi_e - \xi_v) \log_2 \left( 1 + \frac{p_{v,s}^t g_{v,s}}{\sigma^2 + F_s} \right) - \log_2 \left( 1 + \frac{p_{u,s}^{\max} g_{u,s}}{\sigma^2 + F_s} \right) \right). \quad (23)$$

Then, we have

$$\begin{cases} \frac{\mu_s(\xi_e, \xi_v)}{\partial(\xi_v)} = \psi_e WT_v^{\max} (A'B + AB') \\ \frac{\partial^2 \mu_s(\xi_e, \xi_v)}{\partial(\xi_v)^2} = \psi_e WT_v^{\max} (A''B + 2A'B' + AB'') \end{cases}. \quad (24)$$

In (23) and (24),  $A''B$ ,  $2A'B'$ , and  $AB''$  can be obtained by calculating the first and second derivatives of  $A$ , and the first and second derivatives of  $B$

$$A''B = 0$$

$$AB'' = 0$$

$$2A'B' = -2 \frac{\sum_{v \in S_s} T_v^{\max} \varphi_{v,s} |S_s| W \log_2 \left( 1 + \frac{(p_{v,s}^{\max} - p_{v,s}^t) g_{v,s}}{\sigma^2 + F_s} \right)}{\mu_v^{\max}} \cdot \sum_{\substack{\forall v \in S_s \\ \exists u \in U_v}} \log_2 \left( 1 + \frac{p_{v,s}^t g_{v,s}}{\sigma^2 + F_s} \right) < 0.$$

Therefore,  $\frac{\partial^2 \mu_s(\xi_e, \xi_v)}{\partial(\xi_v)^2} < 0$  so that the net utility function defined in (12) is a concave function with respect to  $\xi_v$ . Therefore, let  $\frac{\partial \mu_s(\xi_e, \xi_v)}{\partial \xi_v} = 0$ , the suboptimal response strategy  $\xi_v^*$  of the SBS  $s$  can be solved in theory.

Then, let  $\xi_v$  be fixed as the value  $\xi_v^*$  and demonstrate whether the net utility function defined in (12) is a concave function with respect to  $\xi_e$  or not. The proving process is similar to the proving process of  $\xi_v$ . It is easy to verify that  $\frac{\partial^2 \mu_s(\xi_e, \xi_v^*)}{\partial(\xi_e)^2} < 0$  so that the net utility function defined in (12) is a concave function with respect to  $\xi_e$ . Therefore, let  $\frac{\partial \mu_s(\xi_e, \xi_v^*)}{\partial \xi_e} = 0$ , the suboptimal response strategy  $\xi_e^*$  of the SBS  $s$  can be solved in theory.

Therefore, the optimization problem (17) always has the suboptimal solution  $\{\xi_e^*, \xi_v^*\}$ . That is the end of the proof.

### APPENDIX C PROOF OF THEOREM 4

Let

$$f_D(p_{e,v}^t) = T_e^{\max} \xi_e W \log_2 \left( 1 + \frac{(p_e^{\max} - p_{e,v}^t) g_{e,s}}{\sigma^2 + F_s} \right)$$

$$\text{and } f_I(p_{e,v}^t) = \frac{\log_2 \left( 1 + \frac{\eta_{e,v} p_{e,v}^t g_{e,v}}{\sigma^2 + F_s} \right)}{\Phi_e + \sum_{e' \in R_v} \log_2 \left( 1 + \frac{\eta_{e',v} p_{e',v}^t g_{e',v}}{\sigma^2 + F_s} \right)}. \quad \text{Therefore,}$$

$\mu_e(P_e) = f_D(p_{e,v}^t) f_I(p_{e,v}^t)$ . For simplicity, without loss of generality,  $\mu_e(P_e) = f_D(p_e) f_I(p_e)$ .

By applying the asserted OPF in (18), we first have that

$$\begin{aligned} \Delta \mu_e &= \mu_e(p_e, P_{-e}) - \mu_e(q_e, P_{-e}) \\ &= f_D(p_e) f_I(p_e) - f_D(q_e) f_I(q_e). \end{aligned}$$

Similarly,

$$\begin{aligned} \Delta F &= F(p_e, P_{-e}) - F(q_e, P_{-e}) \\ &= \sum_{e=1}^{|R_v|} \mu_e(p_e, P_{-e}) - \sum_{e=1}^{|R_v|} \mu_e(q_e, P_{-e}) \\ &= \sum_{e=1}^{|R_v|} (f_D(p_e) f_I(p_e) - f_D(q_e) f_I(q_e)). \end{aligned}$$

Therefore, the sign of  $\Delta F$  is same as that of  $\Delta \mu_e$ , which shows that  $F(P_e)$  is an OPF and  $\Theta = \langle \Omega, A, \mu \rangle$  is an OPG according to Definition 2.

### REFERENCES

- [1] Cisco visual networking index: Forecast and methodology, 2016–2021, CISCO, San Jose, CA, USA, White Paper, 2017.
- [2] Z. T. Li, B. M. Chang, S. G. Wang, A. F. Liu, F. Z. Zeng, and G. M. Luo, "Dynamic compressive wide-band spectrum sensing based on channel energy reconstruction in cognitive Internet of Things," *IEEE Trans Ind. Informat.*, vol. 14, no. 6, pp. 2598–2607, Jun. 2018.
- [3] X. Liu, Y. X. Liu, A. F. Liu, and L. T. Yang, "Defending on-off attacks using light probing messages in smart sensors for industrial communication systems," *IEEE Trans. Ind. Informat.*, vol. 14, no. 9, pp. 3801–3811, Sep. 2018.
- [4] The Business Research Company, "Wearable medical devices global market opportunities and strategies to 2022," Rep. ID 5482373, Jul. 2018. [Online]. Available: <https://www.reportlinker.com/p05482373>
- [5] J. S. Gui, L. H. Hui, and N. X. Xiong, "Enhancing cellular coverage quality by virtual access point and wireless power transfer," *Wireless Commun. Mobile Comput.*, vol. 2018, 2018, Art. no. 9218239, doi: 10.1155/2018/9218239.
- [6] L. Xiao, P. Wang, D. Niyato, D. Kim, and Z. Han, "Wireless networks with RF energy harvesting: A contemporary survey," *IEEE Commun. Surv. Tut.*, vol. 17, no. 2, pp. 757–789, Second Quarter 2015.
- [7] Y. W. Liu, L. F. Wang, S. A. R. Zaidi, M. ElKashlan, and T. Q. Duong, "Secure D2D communication in large-scale cognitive cellular networks: A wireless power transfer model," *IEEE Trans. Commun.*, vol. 64, no. 1, pp. 329–342, Jan. 2016.
- [8] H. Chen, Y. Y. Ma, Z. H. Lin, Y. H. Li, and B. Vucetic, "Distributed power control in interference channels with QoS constraints and RF energy harvesting: A game-theoretic approach," *IEEE Trans. Veh. Technol.*, vol. 65, no. 12, pp. 10063–10069, Dec. 2016.
- [9] B. Khalfi, B. Hamdaoui, M. B. Ghorbel, M. Guizani, X. Zhang, and N. Zorba, "Optimizing joint data and power transfer in energy harvesting multiuser wireless networks," *IEEE Trans. Veh. Technol.*, vol. 66, no. 12, pp. 10989–11000, Dec. 2017.
- [10] K. Liang, L. Q. Zhao, K. Yang, X. L. Chu, "Online power and time allocation in MIMO uplink transmissions powered by RF wireless energy transfer," *IEEE Trans. Veh. Technol.*, vol. 66, no. 8, pp. 6819–6830, Aug. 2017.
- [11] L. Zhao and X. D. Wang, "Massive MIMO downlink for wireless information and energy transfer with energy harvesting receivers," *IEEE Trans. Commun.*, vol. 67, no. 5, pp. 3309–3322, May 2019.
- [12] J. C. Kwan and A. O. Fapojuwo, "Radio frequency energy harvesting and data rate optimization in wireless information and power transfer sensor networks," *IEEE Sensors J.*, vol. 17, no. 15, pp. 4862–4874, Aug. 2017.
- [13] K. W. Choi, P. A. Rosyady, L. Ginting, A. A. Aziz, D. Setiawan, and D. I. Kim, "Theory and experiment for wireless-powered sensor networks: How to keep sensors alive," *IEEE Trans. Wireless Commun.*, vol. 17, no. 1, pp. 430–444, Jan. 2018.
- [14] Y. Alsaba, S. K. A. Rahim, and C. Y. Leow, "Beamforming in wireless energy harvesting communications systems: A survey," *IEEE Commun. Surv. Tut.*, vol. 20, no. 2, pp. 1329–1360, Second Quarter 2018.

- [15] S. T. Guo, Y. W. Shi, Y. Y. Yang, and B. Xiao, "Energy efficiency maximization in mobile wireless energy harvesting sensor networks," *IEEE Trans. Mobile Comput.*, vol. 17, no. 7, pp. 1524–1537, Jul. 2018.
- [16] D. Sui, F. Y. Hu, W. Zhou, M. Q. Shao, and M. H. Chen, "Relay selection for radio frequency energy-harvesting wireless body area network with buffer," *IEEE Internet Things J.*, vol. 5, no. 2, pp. 1100–1107, Apr. 2018.
- [17] H. Zhang, Y. X. Guo, Z. Zhong, and W. Wu, "Cooperative integration of RF energy harvesting and dedicated WPT for wireless sensor networks," *IEEE Microw. Wireless Compon. Lett.*, vol. 29, no. 4, pp. 291–293, Apr. 2019.
- [18] D. Altinel and G. K. Kurt, "Modeling of hybrid energy harvesting communication systems," *IEEE Trans. Green Commun. Netw.*, vol. 3, no. 2, pp. 523–534, Jun. 2019.
- [19] J. Ho and M. Jo, "Offloading wireless energy harvesting for IoT devices on unlicensed bands," *IEEE Internet Things J.*, vol. 6, no. 2, pp. 3663–3675, Apr. 2019.
- [20] Z. W. Hou, H. Chen, Y. H. Li, and B. Vucetic, "Incentive mechanism design for wireless energy harvesting-based Internet of Things," *IEEE Internet Things J.*, vol. 5, no. 4, pp. 2620–2632, Aug. 2018.
- [21] Q. Z. Yao *et al.*, "Crowdsourcing in wireless-powered task-oriented networks: Energy bank and incentive mechanism," *IEEE Trans. Wireless Commun.*, vol. 17, no. 12, pp. 7834–7848, Dec. 2018.
- [22] D. Fudenberg and J. Tirole, *Game theory*. Cambridge, MA, USA: MIT Press, 1993.
- [23] D. Monderer and L. Shapley, "Potential games," *Games Econ. Behav.*, vol. 14, pp. 124–143, 1996.
- [24] R. S. Komali, A. B. MacKenzie, and R. P. Gilles, "Effect of selfish node behavior on efficient topology design," *IEEE Trans. Mobile Comput.*, vol. 7, no. 9, pp. 1057–1070, Sep. 2008.
- [25] S. R. Bu and F. R. Yu, "Green cognitive mobile networks with small cells for multimedia communications in the smart grid environment," *IEEE Trans. Veh. Technol.*, vol. 63, no. 5, pp. 2115–2126, Jun. 2014.
- [26] N. Xia, H. H. Chen, and C. S. Yang, "Radio resource management in machine-to-machine communications—A survey," *IEEE Commun. Surv. Tut.*, vol. 20, no. 1, pp. 791–828, First Quarter 2018.
- [27] S. Boyd and L. Vandenberghe, *Convex optimization*. Cambridge, U.K.: Cambridge Univ. Press, 2004.



**Jinsong Gui** (Member, IEEE) received the B.E. degree from the University of Shanghai for Science and Technology, Shanghai, China, in 1992, and the M.S. and Ph.D. degrees from Central South University, Changsha, China, in 2004 and 2008, respectively.

He is currently a Professor with the School of Computer Science and Engineering, Central South University. He is the author or coauthor of more than 50 international journal papers and more than ten international conference papers.

His current research interests include the general area of distributed systems, as well as related fields such as wireless network topology control, cloud and green computing, and network trust and security.

Prof. Gui is a Member of the China Computer Federation (CCF).



**Neal N. Xiong** (Senior Member, IEEE) received the Ph.D. degree in sensor system engineering from Wuhan University, Wuhan, China, in 2007, and the Ph.D. degree in dependable communication networks from the Japan Advanced Institute of Science and Technology, Nomi, Japan, in 2008.

He is currently an Associate Professor (fifth year) with the Department of Mathematics and Computer Science, Northeastern State University, Tahlequah, OK, USA. Prior to this, for about 10 year, he was with Georgia State University, Atlanta, GA, USA, Wentworth Technology Institution, Boston, MA, USA, and Colorado Technical University, Colorado Springs, CO, USA where he was a Full Professor for about 5 year. He is the author or coauthor of more than 200 international journal papers and more than 100 international conference papers. Some of his works were published in the IEEE JOURNAL ON SELECTED AREAS IN COMMUNICATIONS, IEEE/ACM TRANSACTIONS, ACM Sigcomm Workshop, IEEE International Conference on Computer Communications, International Conference on Distributed Computing Systems, and International Parallel and Distributed Processing Symposium. His research interests include cloud computing, security and dependability, parallel and distributed computing, networks, and optimization theory.

Prof. Xiong has been a Senior Member of the IEEE Computer Society since 2012.



**Lihuan Hui** is currently working toward the master's degree in computer science with the School of Computer Science and Engineering, Central South University, Changsha, China.

Her current research interests include the Internet of Things, wireless sensor networks, network simulation, and performance evaluation.



**Jie Wu** (Fellow, IEEE) received the B.S. degree in computer engineering and M.S. degree in computer science from the Shanghai University of Science and Technology (now Shanghai University), Shanghai, China, in 1982 and 1985, respectively, and the Ph.D. degree in computer engineering from Florida Atlantic University, Boca Raton, FL, USA, in 1989.

He is the Director of the Center for Networked Computing and Laura H. Carnell Professor at Temple University, Philadelphia, PA, USA. He was the Chair of the Department of Computer and Information Sciences from the summer of 2009 to the summer of 2016 and Associate Vice Provost for International Affairs from the fall of 2015 to the summer of 2017. He regularly publishes in scholarly journals, conference proceedings, and books. His research interests include mobile computing and wireless networks, routing protocols, cloud and green computing, network trust and security, and social network applications.

Dr. Wu was the recipient of the 2011 China Computer Federation (CCF) Overseas Outstanding Achievement Award. He is a Member of several editorial boards, including the IEEE TRANSACTIONS ON MOBILE COMPUTING, IEEE TRANSACTIONS ON SERVICE COMPUTING, *Journal of Parallel and Distributed Computing*, and *Journal of Computer Science and Technology*. He is a Fellow of the American Association for the Advancement of Science.